0026-895X/07/7204-1054–1062$20.00
MOLECULAR PHARMACOLOGY
Copyright © 2007 The American Society for Pharmacology and Experimental Therapeutics
*Mol Pharmacol* 72:1054–1062, 2007

Vol. 72, No. 4
37952/3257426
*Printed in U.S.A.*



# Critical Roles of Residues 36 and 40 in the Phenol and Tertiary Amine Aglycone Substrate Selectivities of UDP-Glucuronosyltransferases 1A3 and 1A4

Takahiro Kubota,[1] Benjamin C. Lewis, David J. Elliot, Peter I. Mackenzie, and John O. Miners

*Department of Clinical Pharmacology, Flinders University and Flinders Medical Centre, Adelaide, Australia*

Received May 8, 2007; accepted July 16, 2007

## ABSTRACT

Despite high sequence identity, UGT1A3 and UGT1A4 differ in terms of substrate selectivity. UGT1A3 glucuronidates the planar phenols 1-naphthol (1-NP) and 4-methylumbelliferone (4-MU), whereas UGT1A4 converts the tertiary amines lamotrigine (LTG) and trifluoperazine (TFP) to quaternary ammonium glucuronides. Residues 45 to 154 (which incorporate 21 of the 35 amino acid differences) and 45 to 535 were exchanged between UGT1A3 and UGT1A4 to generate UGT1A3-4$_{(45–535)}$, UGT1A3-4$_{(45–154)}$-3, UGT1A4-3$_{(45–535)}$, and UGT1A4-3$_{(45–154)}$-4 hybrid proteins. Although differences in kinetic parameters were observed between the parent enzymes and chimeras, UGT1A4-3$_{(45–535)}$ and UGT1A4-3$_{(45–154)}$-4 [but not UGT1A3-4$_{(45–535)}$ and UGT1A3-4$_{(45–154)}$-3] retained the capacity to glucuronidate LTG and TFP. Likewise, UGT1A3-4$_{(45–535)}$ and UGT1A3-4$_{(45–154)}$-3 retained the capacity to glucuronidate 1-NP and 4-MU, but UGT1A4-3$_{(45–535)}$ and UGT1A4-3$_{(45–154)}$-4 exhibited low or absent activity. Within the first 44 residues, UGT1A3 and UGT1A4 differ in sequence at positions 36 and 40. "Reciprocal" mutagenesis was performed to generate the UGT1A3(I36T), UGT1A3(H40P), UGT1A4(T36I), and UGT1A4 (P40H) mutants. The T36I and P40H mutations in UGT1A4 reduced in vitro clearances for LTG and TFP glucuronidation by >90%. Conversely, the I36T and H40P mutations in UGT1A3 reduced the in vitro clearances for 1-NP and 4-MU glucuronidation by >90%. Introduction of the single H40P mutation in UGT1A3 conferred LTG and TFP glucuronidation, whereas the single T36I mutation in UGT1A4 conferred 1-NP and 4-MU glucuronidation. Thus, residues 36 and 40 of UGT1A3 and UGT1A4 are pivotal for the respective selectivities of these enzymes toward planar phenols and tertiary amines, although other regions of the proteins influence binding affinity and/or turnover.



Glucuronidation involves the covalent linkage of glucuronic acid, derived from the cofactor UDP-glucuronic acid (UDPGA), to a substrate bearing a nucleophilic functional group or atom, most commonly an alcohol (aliphatic or phenolic), amine, or carboxylic acid. Given the widespread occurrence of these functional groups in synthetic and "biological" chemicals, glucuronidation is not surprisingly an essential clearance and detoxification mechanism for a myriad of compounds that include drugs, environmental chemicals, and endogenous compounds particularly bilirubin, fatty acids, and hydroxysteroids (Miners and Mackenzie 1991; Radominska-Pandya et al., 1999). The glucuronidation reaction is catalyzed by the UDP-glucuronosyltransferase (UGT) superfamily of enzymes. Almost 30 *UGT* genes have been identified in humans, and these have been classified in three subfamilies: 1A, 2A, and 2B (Mackenzie et al., 2005). UGT1A and UGT2B enzymes, which are the largest subfamilies, are of greatest importance in the metabolism of xenobiotics and endogenous compounds in humans. It is well established that the individual UGT1A and UGT2B enzymes exhibit distinct but overlapping aglycone substrate selectivities and differ in terms of regulation of expression (Tukey and Strassburg 2000; Radominska-Pandya et al., 1999; Miners et al., 2004; Kiang et al., 2005). However, the structural basis of UGT enzyme substrate selectivity has yet to be fully elucidated.

UGT1A enzymes comprise a unique amino terminus domain of 285 to 289 residues but an identical carboxyl terminus comprising 246 residues that arise from the splicing of

This work was supported by a grant from the National Health and Medical Research Council of Australia. P.I.M. is a National Health and Medical Research Council of Australia Senior Principal Research Fellow. T.K. was supported by an Overseas Study Scholarship from the Japanese Research Foundation.

[1] Current affiliation: Department of Drug Metabolism and Biopharmaceutics, Faculty of Pharmacy, Chiba Institute of Science, Chiba, Japan.

Article, publication date, and citation information can be found at http://molpharm.aspetjournals.org.
doi:10.1124/mol.107.037952.

**ABBREVIATIONS:** UDPGA, UDP-glucuronic acid; UGT, UDP-glucuronosyltransferase; LTG, lamotrigine; TFP, trifluoperazine; 4-MU, 4-methylumbelliferone; 1-NP, 1-naphthol; HEK, human embryonic kidney; HPLC, high-performance liquid chromatography.

individual "first" exons to four common exons (Ritter et al., 1992; Mackenzie et al., 2005). Whereas the conserved carboxyl terminus contributes to cofactor (UDPGA) binding (Radominska-Pandya et al., 1999), the aglycone substrate selectivity of UGT1A enzymes is clearly determined by the amino terminus. Although UGT2B enzymes are encoded by unique genes and therefore differ in sequence throughout the polypeptide chain, studies with chimeric rat, rabbit and human proteins and nuclear magnetic resonance analysis similarly implicate the amino terminus domains of several UGT2B enzymes in substrate binding and selectivity (Mackenzie 1990; Li et al., 1997; Lewis et al., 2007). Mutagenesis has further identified a limited number of amino acids that influence the binding of UGT1A6, UGT1A10, UGT2B15, and UGT2B17 substrates (Dubois et al., 1999; Ouzzine et al., 2000; Senay et al., 2002; Martineau et al., 2004; Xiong et al., 2006; Lewis et al., 2007), and mis-sense mutations arising from genetic polymorphism of both *UGT1A* and *UGT2B* genes are known to alter substrate binding and/or turnover (Miners et al., 2002; Guillemette, 2003).

Within the UGT1A subfamily, UGT1A3 and UGT1A4 differ in sequence by only 35 amino acids (Fig. 1). Despite sharing 93.4% sequence identity, however, UGT1A3 and UGT1A4 differ markedly in terms of substrate selectivity. It is noteworthy that only UGT1A4 converts tertiary amines such as lamotrigine (LTG) and trifluoperazine (TFP) (see Fig. 2 for structures) to a quaternary ammonium glucuronide (Green and Tephly, 1998; Green et al., 1998; Rowland et al., 2006; Uchaipichat et al., 2006). Conversely, UGT1A4 lacks activity toward the planar phenols 4-methylumbelliferone (4-MU) and 1-naphthol (1-NP) (see Fig. 2 for structures), whereas UGT1A3 and indeed most other human UGTs catalyze the glucuronidation of these compounds (Green et al., 1998; Uchaipichat et al., 2004).

The high sequence identity of UGT1A3 and UGT1A4 provides a convenient experimental model for probing the structural basis for the differing substrate selectivities of UGT enzymes. The majority of the amino acid differences between UGT1A3 and UGT1A4 occur between positions 47 and 127 (Fig. 1). Based on the chimeragenesis approach adopted in this laboratory to identify the substrate binding domain of UGT2B15 (Lewis et al., 2007), we used common SphI and HpaI restriction sites in the UGT1A3 and UGT1A4 cDNAs to generate UGT1A3-4$_{(45–535)}$, UGT1A3-4$_{(45–154)}$-3, UGT1A4-3$_{(45–535)}$ and UGT1A4-3$_{(45–154)}$-4 chimeras. Substrate selectivity was assessed using LTG, TFP, 4-MU, and 1-NP as the model substrates (Fig. 2). After demonstration that substrate selectivity was associated with the first 44 amino acids of each enzyme, the two residues (36 and 40) that differ in this region of the mature protein were subsequently shown to be critical for the respective selectivities of UGT1A3 and UGT1A4.

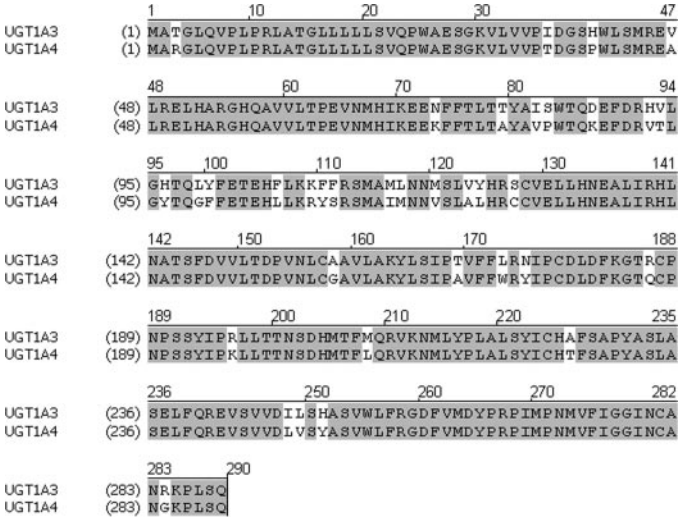


**Fig. 1.** Amino acid alignment of UGT1A3 and UGT1A4. Identical residues are shaded gray. Residues 285 to 534 are identical; hence, sequence beyond position 290 is not shown. Overall, the UGT1A3 and UGT1A4 proteins share 93.4% sequence identity and 95.9% similarity.

## Materials and Methods

### Materials

LTG and lamotrigine N2-glucuronide were obtained from the Wellcome Research Laboratories (Beckenham, UK). 4-MU, 4-methylumbelliferone-β-D-glucuronide, 1-naphthol (1-NP), 1-naphthol-β-D-glucuronide, TFP (dihydrochloride salt), and UDPGA (trisodium salt) were purchased from Sigma-Aldrich (Sydney, Australia). *Pfu* Ultra Polymerase was from Stratagene (La Jolla, CA), and restriction enzymes were supplied by New England Biolabs (Ipswich, MA). Dulbecco's modified Eagle's medium, minimal essential medium nonessential amino acids (10 mM), and penicillin/streptomycin solution (penicillin-G, 5000 U/ml; streptomycin sulfate, 5000 mg/ml) were purchased from Invitrogen (Carlsbad, CA). Other reagents and organic solvents were of analytical reagent grade. The UGT1A3 and UGT1A4 cDNAs were isolated as described previously (Mojarrabi et al., 1996; Uchaipichat et al., 2004).

### Methods

**Generation of Chimeric and Mutant UGT cDNAs.** The UGT1A3 and UGT1A4 cDNAs (accession numbers NM_019093 and NM_007120, respectively) were independently subcloned into pBluescript-II-SK(+) (Stratagene, La Jolla, CA) for DNA manipulation. Parental templates, which are of equal length, were used to generate four UGT1A3/1A4 chimeras, namely UGT1A3-4$_{(45–535)}$ (referred to subsequently as UGT1A3-4), UGT1A3-4$_{(45–154)}$-3 (referred to subsequently as UGT1A3-4-3), UGT1A4-3$_{(45–535)}$ (referred to subsequently as UGT1A4-3), and UGT1A4-3$_{(45–154)}$-4 (referred to subsequently as UGT1A4-3-4) according to the strategy shown in Fig. 3. Digestion of the parental templates with SphI and NotI gave a 1487-base pair

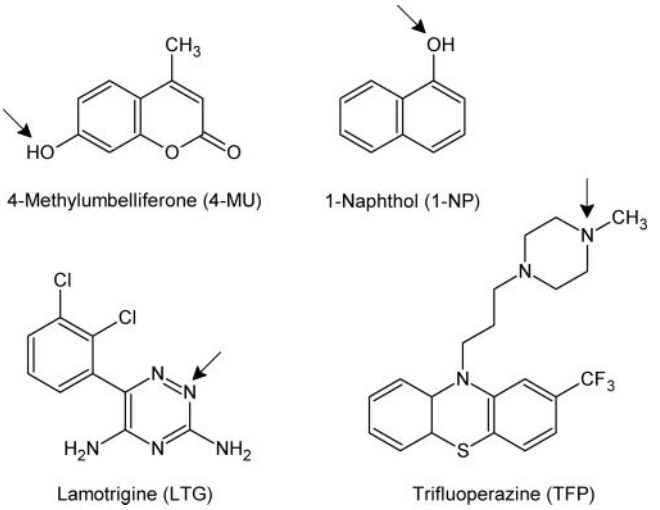


**Fig. 2.** Structures of lamotrigine (LTG), trifluoperazine (TFP), 1-naphthol (1-NP), and 4-methylumbelliferone (4-MU). Arrows indicate the primary sites of glucuronidation.

fragment (encoding residues 45–534) that was exchanged between the parental templates to generate the UGT1A3-4 and UGT1A4-3 cDNAs. Likewise, the UGT1A3-4-3 and UGT1A4-3-4 chimeras were generated by exchanging the 330-base pair fragment (encoding residues 45–154) obtained by digestion of the parental templates with SphI and HpaI. UGT1A3(I36T), UGT1A3(H40P), UGT1A4(T36I), and UGT1A4(P40H) were generated by reciprocal mutagenesis at positions 36 and 40 of the UGT1A3 and UGT1A4 cDNA templates. Mutants were engineered using the QuikChange-II site-directed mutagenesis protocol (Stratagene) with the oligonucleotide primers shown in Table 1. After digestion with XhoI and NotI (Fig. 3), coding sequences were subcloned into the mammalian expression vector pEF-IRES-puro6 for transfection into HEK293 cells (Uchaipichat et al., 2004). All DNA manipulations were confirmed on both strands by direct sequencing (ABI PRISM 3100; Applied Biosystems, Foster City, CA).

**Expression of UGT Enzymes, Chimeras and Mutants.** The UGT1A3, UGT1A4, UGT1A3-4, UGT1A3-4-3, UGT1A4-3, UGT1A4-3-4, UGT1A3(I36T), UGT1A3(H40P), UGT1A4(T36I) and UGT1A4(P40H) cDNAs were stably expressed in the human embryonic kidney cell line, HEK293. After transfection, cells were incubated in a humidified incubator with an atmosphere of 5% $CO_2$ at 37°C in Dulbecco's modified Eagle's medium prepared in the presence of sodium bicarbonate (44 mM), minimal essential medium nonessential amino acids (0.1 mM), fetal bovine serum (10%), and penicillin/streptomycin (100 U/ml). Media were supplemented with puromycin (1.0 mg/l) for selection. Cells were grown to no more than 90% confluence. The conditioned medium was decanted, and the cultured cells were washed (three times) with prechilled (4°C) phosphate-buffered saline, pH 7.4. Cell pellets were resuspended in a storage buffer (10 mM $K_2HPO_4/KH_2PO_4$, pH 7.4, and 0.1 mM EDTA) and kept at −80°C until use. Cells were lysed using the sonication method described by Uchaipichat et al. (2004).

**Enzyme Assays.** Substrate concentration ranges were determined from initial activity screening experiments (four concentrations) to permit reliable identification of the glucuronidation kinetic model and kinetic constants for each protein source. Incubation conditions were optimized for linearity with respect to both protein concentration and incubation time. Details of individual assays, based on methods established in this laboratory, are provided below.

4-MU and 1-NP glucuronidation. Incubation mixtures contained UDPGA (5 mM), $MgCl_2$ (4 mM), HEK293 cell lysate expressing each recombinant UGT1A protein (0.5 mg/ml), phosphate buffer (0.1 M, pH 7.4), and 4-MU or 1-NP (9–11 concentrations) in a total volume of 0.2 ml. Incubations were conducted in air at 37°C for 75 (4-MU) or 120 (1-NP) min, after which time reactions were terminated by the addition of perchloric acid (70%; 3 $\mu$l) and cooling on ice. 4-Methylumbelliferone-$\beta$-D-glucuronide and 1-naphthol-$\beta$-D-glucuronide were separated and quantified according to the HPLC methods reported by Udomuksorn et al. (2007).

LTG N2-glucuronidation. The incubation mixture, in a total volume of 0.2 ml, contained UDPGA (5 mM), $MgCl_2$ (4 mM), HEK293 cell lysate expressing each recombinant UGT1A protein (0.5 mg/ml), and LTG (10 concentrations). Because of its limited solubility LTG was dissolved in 1 M phosphoric acid containing 10% acetonitrile. Phosphate buffer (0.1 M, pH 7.4) was generated in situ by the addition of KOH (1 M, 37.2 $\mu$l). Incubations were performed in air at 37°C for 75 min. Reactions were terminated by the addition of 70% perchloric acid (3 $\mu$l) and cooling on ice, and the LTG N2-glucuronide was separated and quantified according to the HPLC procedure of Rowland et al. (2006).

TFP glucuronidation. Incubations contained UDPGA (5 mM), $MgCl_2$ (4 mM), HEK293 cell lysate expressing each recombinant UGT1A protein (0.25 mg/ml), 50 mM Tris-HCl buffer, pH 7.4, and TFP (10 concentrations). Incubations were conducted in air at 37°C for 20 min, after which time reactions were terminated by the addition of 4% acetic acid/96% methanol (0.2 ml) and cooling on ice. TFP glucuronide was separated and quantified by HPLC as described by Uchaipichat et al. (2006).

All incubations were performed in duplicate, and data points represent the mean of duplicate measurements (<10% difference). Overall within-day assay reproducibility for each procedure was assessed by measuring the rate of glucuronide formation in 8 to 10 separate incubations with either UGT1A3 or UGT1A4 as the enzyme source. Coefficients of variation, determined for both "low" and "high" substrate concentrations with each assay, were <7.3%. Limits of quantification, expressed as rates of glucuronide formation, were 1.5, 1.0, 0.7, and 0.5 pmol/min/mg for the TFP, LTG, 4-MU, and 1-NP glucuronidation assays, respectively.

**Immunoblotting.** Twenty micrograms of HEK293 cell lysate protein was subjected to 10% SDS-polyacrylamide gel electrophoresis and electrophoretically transferred onto nitrocellulose (Bio-Rad Laboratories, Hercules, CA). Blots were probed with an anti- UGT1A antibody (diluted 1:1500; BD Gentest, Woburn, MA) that recognizes an epitope in the conserved carboxyl-terminal domain of UGT1A proteins followed by goat anti-rabbit IgG coupled to horseradish peroxidase (diluted 1:3000; Southern Biotechnology Associates, Birmingham, AL). Proteins were visualized by chemiluminescence (enhanced chemiluminescence-plus; GE Healthcare, Chalfont St. Giles, Buckinghamshire, UK) and band intensities were determined with a Bio-Rad model GS-700 imaging densitometer. Relative expression levels reported under *Results* represent the mean of duplicate experiments (< 10% variance).

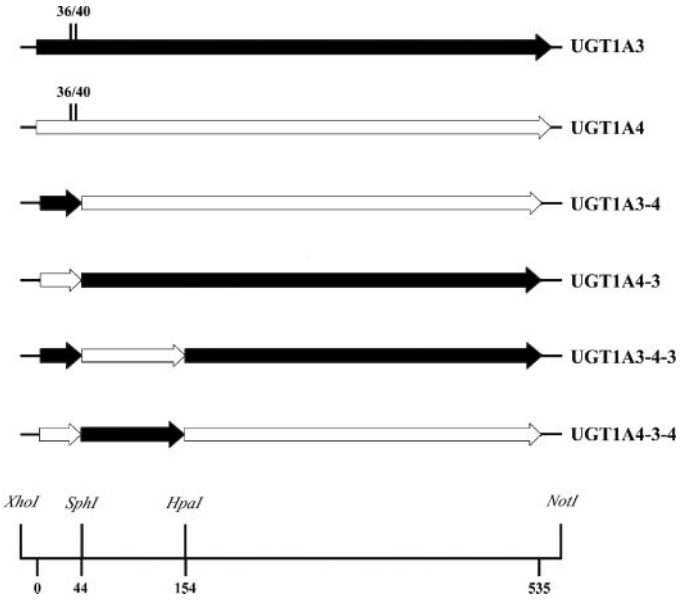


**Fig. 3.** Construction of the UGT1A3-UGT1A4 chimeras. Arrow heads show the junctions between various UGT1A3 and UGT1A4 coding sequences. 5′- to 3′-XhoI and NotI restriction sites flank the entire UGT1A3 and UGT1A4 coding sequences and were used in the directional transfer of cDNAs into the mammalian expression vector pEF-IRESpuro6. SphI and HpaI restriction sites were employed to construct chimeric cDNAs that result in exchange of residues 45 to 154 and 45 to 535 of UGT1A3 and UGT1A4.

TABLE 1
Oligonucleotides used for the construction of the UGT1A3 and UGT1A4 mutants at residues 36 and 40

Mutagenized positions are underlined. Accession numbers for UGT1A3 and UGT1A4 are AY435138.1 and AY435139.1, respectively.

| Mutant | Primers |
|---|---|
| UGT1A3(I36T) | 5′-GTGTTGGTGGTGCCCAC<u>T</u>GATGGCAGCCACTGG-3′ |
| UGT1A3(H40P) | 5′-CCCATTGATGGCAGCC<u>C</u>CTGGCTCAGCATGCGG-3′ |
| UGT1A4(T36I) | 5′-GGTGTTGGTGGTGCCCA<u>T</u>TGATGGCAGCCCCTG-3′ |
| UGT1A4(P40H) | 5′-CCCACTGATGGCAGCC<u>A</u>CTGGCTCAGCATGCGG-3′ |

**Data Analysis.** Kinetic constants for 4-MU, 1-NP, LTG, and TFP glucuronidation by each recombinant protein, including chimeras and mutants, were obtained by fitting untransformed data to the following models using Enzfitter (Biosoft, Cambridge, UK).

*Michaelis-Menten equation.*

$$v = \frac{V_{max} \times [S]}{K_m + [S]} \quad (1)$$

where $v$ is the rate of reaction, $V_{max}$ is the maximum velocity, $K_m$ is the Michaelis-Menten constant (substrate concentration at 0.5 $V_{max}$), and [S] is the substrate concentration.

*Substrate inhibition.*

$$v = \frac{V_{max}}{1 + (K_m/[S]) + ([S]/K_{si})} \quad (2)$$

where $K_{si}$ is the constant describing the substrate inhibition interaction.

*The Hill equation,* which describes sigmoidal kinetics:

$$v = \frac{V_{max} \times [S]^{n_H}}{S_{50} + [S]^{n_H}}$$

where $S_{50}$ is the substrate concentration resulting in 50% of $V_{max}$ (analogous to $K_m$ in previous equations) and $n_H$ is the Hill coefficient.

For reactions exhibiting Michaelis-Menten and substrate inhibition kinetics, intrinsic clearance ($CL_{int}$) was calculated as $V_{max}/K_m$. Autoactivation is characterized by the dependence of clearance on substrate concentration. For reactions exhibiting sigmoidal kinetics, maximum clearance provides an alternative estimate of the highest clearance attained [that is, when the enzyme is fully activated before saturation occurs (Houston and Kenworthy 2000)]. $CL_{max}$ was determined as:

$$CL_{max} = \frac{V_{max}}{S_{50}} \times \frac{(n_H - 1)}{n_H(n_H - 1)^{1/n_H}} \quad (3)$$

Goodness of fit to kinetic and inhibition models was assessed from the $F$ statistic, $r^2$ values, parameter standard error estimates, and 95% confidence intervals. Each kinetic constant is presented as the value ± S.E. of the parameter estimate. Kinetic curves are shown as Eadie-Hofstee plots from fitting to the Michaelis-Menten, substrate inhibition, and Hill equations.

## Results

Expression of UGT1A3, UGT1A4 and the UGT1A3/4 chimeras is shown in Fig. 4. Relative expression levels of UGT1A3, UGT1A3-4, UGT1A3-4-3, UGT1A4, UGT1A4-3, and UGT1A4-3-4 were 1, 0.74, 0.73, 0.69, 1.02, and 1.18, respectively. Given the differences in expression of the chimeras relative to the parent enzymes, activities reported throughout this article have been normalized for expression relative to UGT1A3 to permit comparison of $V_{max}$ values and in vitro clearances ($CL_{int}$ and $CL_{max}$).

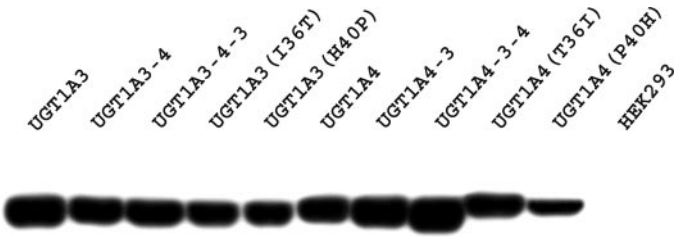


**Fig. 4.** Immunoblot analysis of the parent, chimeric, and mutant UGT1A3 and UGT1A4 recombinant proteins. Twenty micrograms of cell lysate protein was resolved by SDS-polyacrylamide gel electrophoresis, transferred to nitrocellulose, and probed with anti-UGT1A antiserum. Immunoreactive bands occur at 56 to 58 kDa.

Consistent with previous reports, UGT1A4, but not UGT1A3, glucuronidated LTG and TFP. Of the chimeras, UGT1A4-3 and UGT1A4-3-4 glucuronidated LTG and TFP, whereas UGT1A3-4 and UGT1A3-4-3 lacked activity toward these substrates. Kinetic constants for LTG and TFP glucuronidation by UGT1A4, UGT1A4-3, and UGT1A4-3-4 are shown in Tables 2 and 3, respectively, whereas kinetic plots for LTG (as the "model" tertiary amine substrate) glucuronidation by UGT1A4 and these chimeras are illustrated in Fig. 5. In vitro clearances for LTG glucuronidation by UGT1A4, UGT1A4-3, and UGT1A4-3-4 varied approximately 2-fold (0.70–1.34 μl/min/mg), although it should be noted that $CL_{int}$ and $CL_{max}$ are not equivalent parameters. In contrast to the Michaelis-Menten kinetics observed with UGT1A4 and UGT1A4-3, LTG glucuronidation by UGT1A4-3-4 exhibited sigmoidal kinetics (modeled by the Hill equation) (Fig. 5); $K_m$ (or $S_{50}$) and $V_{max}$ values differed between each protein (Table 2). TFP glucuronidation by UGT1A4-3 and UGT1A4-3-4 also exhibited sigmoidicity in contrast to the substrate inhibition kinetics observed for TFP metabolism by UGT1A4 (Table 3). $V_{max}$ values for TFP glucuronidation by the chimeras were lower than that observed for UGT1A4 resulting in lower in vitro clearances (Table 3). Again, however, caution should be exercised in comparing $CL_{int}$ and $CL_{max}$ values for TFP glucuronidation by UGT1A4 and the chimeras. The Michaelis-Menten and substrate inhibition kinetics observed for UGT1A4 catalyzed glucuronidation of LTG and TFP, respectively, are consistent with published data from this laboratory (Rowland et al., 2006; Uchaipichat et al., 2006).

UGT1A3, but not UGT1A4, glucuronidated 1-NP and 4-MU, and the substrate inhibition kinetics observed with both substrates are consistent with previous data from this laboratory (Uchaipichat et al., 2004). Of the chimeras, 1-NP was metabolized only by UGT1A3-4 and UGT1A3-4-3. However, UGT1A3-4, UGT1A3-4-3, UGT1A4-3, and UGT1A4-3-4 all glucuronidated 4-MU, although the in vitro clearances of the latter two chimeras were low compared with UGT1A3, UGT1A3-4, and UGT1A3-4-3. Kinetic constants for 1-NP and

TABLE 2

Derived kinetic constants for LTG glucuronidation by UGT1A3 and UGT1A4 chimeras and mutants

Data shown as parameters ± S.E. of parameter fit.

| Enzyme | $K_m$[a,b] or $S_{50}$[c] | $V_{max}$[d] | $CL_{int}$[e] or $CL_{max}$[f] |
|---|---|---|---|
| | *μM* | *pmol/min/mg* | *μl/min. mg* |
| UGT1A3 | N.A. | N.A. | N.A. |
| UGT1A3–4 | N.A. | N.A. | N.A. |
| UGT1A3–4-3 | N.A. | N.A. | N.A. |
| UGT1A3(I36T) | N.A. | N.A. | N.A. |
| UGT1A3(H40P) | 235 ± 8[a] | 203 ± 1 | 0.86 |
| UGT1A4 | 1162 ± 44[a] | 803 ± 9 | 0.70 |
| UGT1A4–3 | 341 ± 4[a] | 460 ± 2 | 1.34 |
| UGT1A4–3-4 | 1422 ± 21[c] | 2520 ± 26 | 0.98 |
| UGT1A4(T36I) | N.A. | N.A. | N.A. |
| UGT1A4(P40H) | 1105 ± 10[b] | 63 ± 0.3 | 0.06 |

N.A., no activity.
[a] From fitting to the Michaelis Menten equation.
[b] From fitting to the substrate inhibition equation ($K_{si}$ = 7695 ± 267 μM).
[c] From fitting to the Hill equation ($n$ = 1.38 ± 0.02).
[d] Normalized for expression relative to UGT1A3.
[e] Calculated as $V_{max}/K_m$.
[f] Calculated according to eq. 4.

4-MU glucuronidation by UGT1A3 and the chimeras are shown in Tables 4 and 5, respectively, whereas kinetic plots for 1-NP (as the model phenolic substrate) glucuronidation by UGT1A3 and chimeras are illustrated in Fig. 6. Substrate inhibition kinetics were observed for 1-NP and 4-MU metabolism by the chimeras, except for 1-NP glucuronidation by UGT1A3-4 (Michaelis-Menten) and 4-MU glucuronidation by UGT1A4-3 (sigmoidal) (Tables 4 and 5, Fig. 6). Whereas $CL_{int}$ values for 4-MU glucuronidation by UGT1A3, UGT1A3-4, and UGT1A3-4-3 were similar (0.87–1.06 μl/min/mg) (Table 5), $CL_{int}$ values for 1-NP glucuronidation by the respective chimeras were 8.5- and 3-fold higher than the $CL_{int}$ determined for UGT1A3 (Table 4). However, $K_m$ values for both substrates were lower for the chimeras compared with UGT1A3.

TABLE 3

Derived kinetic parameters for TFP glucuronidation by UGT1A3 and UGT1A4 chimeras and mutants

Data shown as parameters ± S.E. of parameter fit.

| Enzyme | $K_m$ [a] or $S_{50}$ [b] | Hill Coefficient ($n_H$) [b] | $V_{max}$ [c] | $CL_{int}$ [d] or $CL_{max}$ [e] |
|---|---|---|---|---|
| | μM | | pmol/min/mg | μl/min/mg |
| UGT1A3 | N.A. | N.A. | N.A. | N.A. |
| UGT1A3–4 | N.A. | N.A. | N.A. | N.A. |
| UGT1A3–4-3 | N.A. | N.A. | N.A. | N.A. |
| UGT1A3(I36T) | N.A. | N.A. | N.A. | N.A. |
| UGT1A3(H40P) | 31 ± 1[b] | 1.34 ± 0.04 | 121 ± 2 | 2.21 |
| UGT1A4 | 40 ± 1[a] | | 1119 ± 7 | 28 |
| UGT1A4–3 | 58 ± 1[b] | 1.58 ± 0.04 | 46 ± 1 | 0.50 |
| UGT1A4–3-4 | 52 ± 3[b] | 1.62 ± 0.07 | 72 ± 4 | 0.71 |
| UGT1A4(T36I) | N.A. | N.A. | N.A. | N.A. |
| UGT1A4(P40H) | 28 ± 0.8[b] | 1.28 ± 0.03 | 83 ± 2 | 1.75 |

N.A., no activity.
[a] From fitting to the substrate inhibition equation ($K_{si}$ = 241 ± 18 μM).
[b] From fitting to the Hill equation.
[c] Normalized for expression relative to UGT1A3.
[d] Calculated as $V_{max}/K_m$.
[e] Calculated according to eq. 4.

The first 25 residues constitute a signal peptide that is cleaved upon insertion of the UGT protein into the membrane of the endoplasmic reticulum. UGT1A3 and UGT1A4 differ by only two amino acids between positions 26 and 44 (Fig. 1); UGT1A3 has Ile and His at positions 36 and 40, respectively, whereas UGT1A4 has Thr and Pro at these positions. Thus, "reciprocal" mutagenesis was performed, and the capacity of the UGT1A3(I36T), UGT1A3(H40P), UGT1A4(T36I), and UGT1A4(P40H) mutants to glucuronidate LTG, TFP, 1-NP, and 4-MU was determined. Expression of the mutants is shown in Fig. 4; relative expression levels of UGT1A3, UGT1A3(I36T), UGT1A4(H40P), UGT1A4(T36I), and UGT1A4(P40H) were 1, 0.59, 0.49, 0.75, and 0.41.

The T36I mutation in UGT1A4 abolished activity toward LTG and TFP, whereas the P40H mutation reduced the in vitro clearances for the glucuronidation of these substrates by an order of magnitude and altered the kinetic model for LTG/TFP glucuronidation (Tables 2 and 3, Fig. 5). Likewise, the I36T mutation in UGT1A3 reduced the in vitro clearances for 1-NP and 4-MU glucuronidation by 92 to 94%,

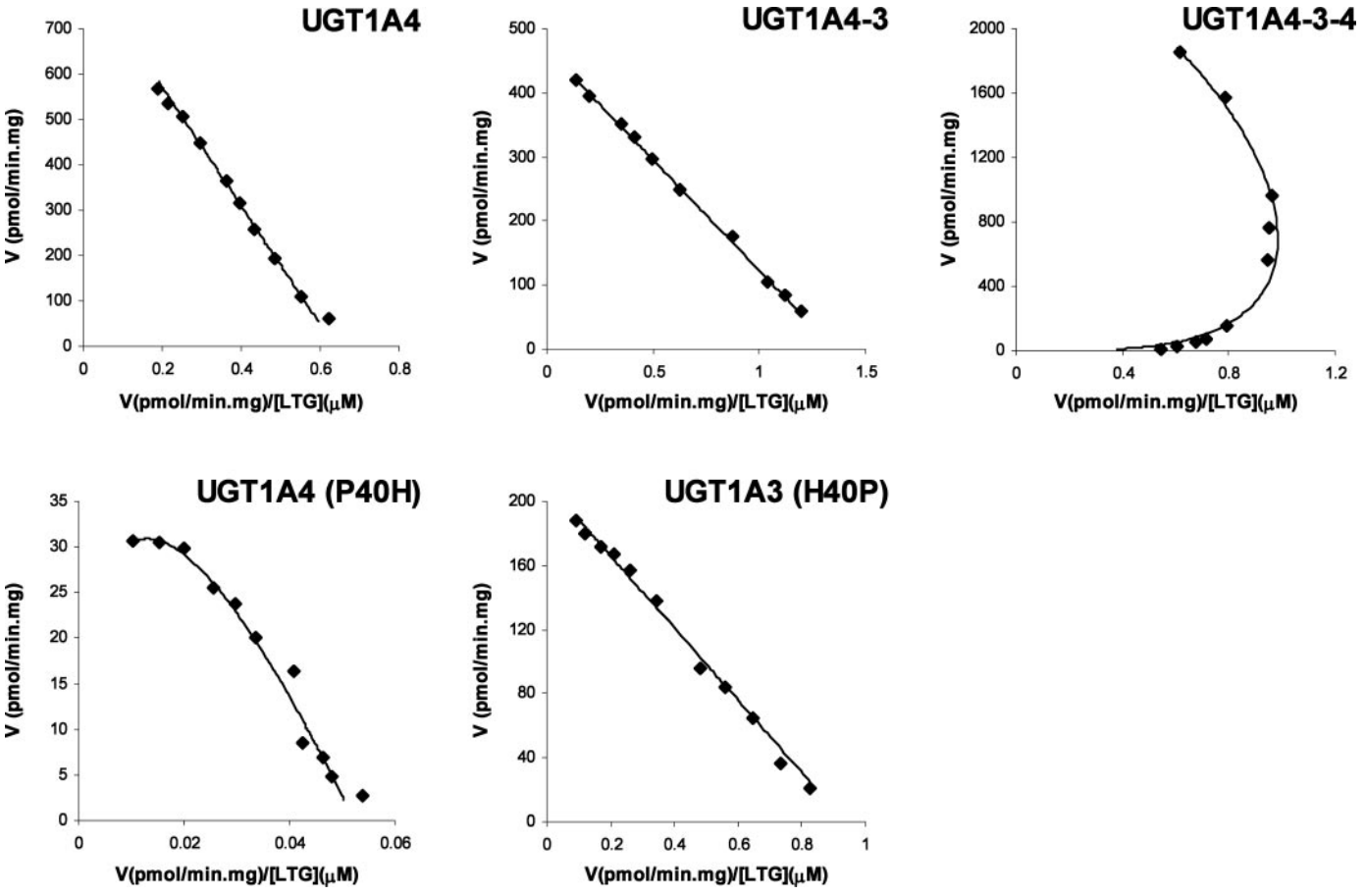


**Fig. 5.** Eadie-Hofstee plots for LTG glucuronidation by UGT1A4, UGT1A4-3, UGT1A4-3-4, UGT1A4(P40H), and UGT1A3(H40P). Points show experimentally determined values (mean of duplicate estimates), whereas curves are the computer-generated curves of best fit.

whereas the H40P mutation essentially abolished the metabolism of these compounds (Tables 4 and 5). Substitution of Pro for His at position 40 of UGT1A3, but not Thr for Ile at position 36, conferred tertiary amine glucuronidation activity. The $CL_{int}$ values for LTG glucuronidation by UGT1A3(H40P) and UGT1A4 were close in value, although both the $K_m$ and $V_{max}$ were lower for the mutant (Table 2). Like UGT1A4, LTG glucuronidation by UGT1A3(H40P) followed Michaelis-Menten kinetics, whereas TFP glucuronidation by this mutant exhibited sigmoidal kinetics (compared with substrate inhibition observed for UGT1A4). The $CL_{int}$ value for TFP glucuronidation by UGT1A3(H40P) was only 8% of that of UGT1A4, largely because of a decrease in $V_{max}$ (Table 3). Conversely, substitution of Ile for Thr at position 36 of UGT1A4, but not His for Pro at position 40, conferred phenolic glucuronidation activity. The $CL_{int}$ for 1-NP glucuronidation by UGT1A4(T36I) was 6.5-fold higher than that of UGT1A3 (Table 4), whereas the $CL_{int}$ for 4-MU glucuronidation by this mutant was only 17% of that of UGT1A3 as a result of a markedly lower $V_{max}$ (Table 5).

## Discussion

Despite sharing 93.4% sequence identity UGT1A3 and UGT1A4 differ in terms of aglycone substrate selectivity, particularly the capacity to glucuronidate tertiary amines and phenols. Amino acid sequence analysis and studies with chimeric UGT proteins are consistent with the hypothesis that amino-terminal domains are responsible for the unique aglycone substrate selectivities of UGTs (Mackenzie 1990; Li et al., 1999; Radominska-Pandya et al., 1999; Lewis et al., 2007). Recent work from this laboratory demonstrated that UGT2B7-UGT2B15 chimeras that incorporated residues 61 to 194 of UGT2B15 exhibited UGT2B15-like substrate selectivity and glucuronidation kinetics (Lewis et al., 2007). Like UGT2B subfamily proteins, greatest sequence dissimilarity occurs between residues 60 and 190 of UGT1A proteins. Indeed, 21 of the 35 amino acid differences between UGT1A3 and UGT1A4 occur between positions 47 and 127, and we reasoned that this region was responsible for the differing substrate selectivities of the two enzymes.

Thus, residues 45 to 154 and 45 to 535 were exchanged between UGT1A3 and UGT1A4 to generate UGT1A3-4, UGT1A3-4-3, UGT1A4-3, and UGT1A4-3-4 hybrid proteins. Although differences in kinetic parameters were observed between the parent enzymes and chimeras (discussed below), UGT1A4-3 and UGT1A4-3-4 retained the characteristic capacity of UGT1A4 to glucuronidate the tertiary amines LTG and TFP, whereas UGT1A3-4 and UGT1A3-4-3 lacked activity toward these compounds. Likewise, UGT1A3-4 and UGT1A3-4-3 retained the UGT1A3-like capacity to glucuronidate the phenolic substrates 1-NP and 4-MU. UGT1A4-3 and UGT1A4-3-4 also glucuronidated 4-MU (but not 1-NP), although in vitro clearances for 4-MU glucuronidation by these chimeras were an order of magnitude or more lower than for UGT1A3.

Taken together, these data indicate that the domain spanning residues 1 to 44 is critical for the unique substrate selectivities of UGT1A3 and UGT1A4. When it is considered that the first 25 residues constitute a signal peptide that is cleaved upon insertion of the UGT protein into the membrane of the endoplasmic reticulum (Radominska-Pandya et al., 1999), UGT1A3 and UGT1A4 differ by only two amino acids in this domain; Ile (UGT1A3) and Thr (UGT1A4) at position 36 and His (UGT1A3) and Pro (UGT1A4) at position 40 (Fig. 1). To gain insight into the contributions of each of these amino acids to UGT1A3 and UGT1A4 substrate selec-

TABLE 4

Derived kinetic constants for 1-NP glucuronidation by UGT1A3 and UGT1A4 chimeras and mutants

Data shown as parameters ± S.E. of parameter fit.

| Enzyme | $K_m$ [a,b] | $K_{si}$ [a] | $V_{max}$ [c] | $CL_{int}$ [d] |
|---|---|---|---|---|
| | *μM* | *μM* | *pmol/min/mg* | *μl/min/mg* |
| UGT1A3 | 2330 ± 24[a] | 916 ± 13 | 300 ± 2 | 0.13 |
| UGT1A3–4 | 314 ± 2[b] | | 351 ± 1 | 1.12 |
| UGT1A3–4-3 | 342 ± 18[a] | 2207 ± 125 | 127 ± 3 | 0.37 |
| UGT1A3(I36T) | 3399 ± 360[a] | 437 ± 42 | 57 ± 3 | 0.01 |
| UGT1A3(H40P) | N.A. | N.A. | N.A. | N.A. |
| UGT1A4 | N.A. | N.A. | N.A. | N.A. |
| UGT1A4–3 | N.A. | N.A. | N.A. | N.A. |
| UGT1A4–3-4 | N.A. | N.A. | N.A. | N.A. |
| UGT1A4(T36I) | 137 ± 2[b] | - | 116 ± 1 | 0.84 |
| UGT1A4(P40H) | N.A. | N.A. | N.A. | N.A. |

N.A., no activity.
[a] From fitting to the substrate inhibition equation.
[b] From fitting to the Michaelis Menten equation.
[c] Normalized for expression relative to UGT1A3.
[d] Calculated as $V_{max}/K_m$.

TABLE 5

Derived kinetic constants for 4-MU glucuronidation by UGT1A3 and UGT1A4 chimeras and mutants

Data shown as parameters ± S.E. of parameter fit.

| Enzyme | $K_m$ [a] or $S_{50}$ [b] | $K_{si}$ [a] | Hill coefficient ($n_H$) [b] | $V_{max}$ [c] | $CL_{int}$ [d] or $CL_{max}$ [e] |
|---|---|---|---|---|---|
| | *μM* | *μM* | | *pmol/min/mg* | *μl/min/mg* |
| UGT1A3 | 1205 ± 37[a] | 916 ± 30 | | 1273 ± 41 | 1.06[d] |
| UGT1A3–4 | 781 ± 10[a] | 1931 ± 35 | | 767 ± 2 | 0.98[d] |
| UGT1A3–4-3 | 702 ± 71[a] | 1496 ± 193 | | 613 ± 2 | 0.87[d] |
| UGT1A3(I36T) | 994 ± 39[b] | | 1.57 ± 0.06 | 115 ± 1 | 0.06[e] |
| UGT1A3(H40P) | 1493 ± 93[b] | | 2.12 ± 0.15 | 15 ± 0.5 | 0.01[e] |
| UGT1A4 | N.A. | N.A. | N.A. | N.A. | N.A. |
| UGT1A4–3 | 1012 ± 29[b] | | 2.29 ± 0.14 | 24 ± 0.2 | 0.02[e] |
| UGT1A4–3-4 | 848 ± 102[a] | 2393 ± 160 | | 87 ± 11 | 0.10[d] |
| UGT1A4(T36I) | 537 ± 6[a] | 1680 ± 32 | | 98 ± 1 | 0.18[d] |
| UGT1A4(P40H) | N.A. | N.A. | N.A. | N.A. | N.A. |

N.A., no activity.
[a] From fitting to the substrate inhibition equation.
[b] From fitting to the Hill equation.
[c] Normalized for expression relative to UGT1A3.
[d] Calculated as $V_{max}/K_m$.
[e] Calculated according to eq. 4.

tivity, reciprocal mutagenesis was performed to generate the UGT1A3(I36T), UGT1A3(H40P), UGT1A4(T36I), and UGT1A4(P40H) mutants. The T36I mutation in UGT1A4 abolished LTG and TFP glucuronidation, whereas the P40H substitution reduced the in vitro intrinsic clearances for LTG and TFP glucuronidation by more than 90%. Conversely, the H40P mutation in UGT1A3 essentially abolished 1-NP and 4-MU glucuronidation, whereas the I36T substitution reduced the in vitro intrinsic clearances for the glucuronidation of these substrates by approximately 95%. Consistent with the critical roles of both positions, the double I36T/H40P mutation (i.e., UGT1A4-3) in the mature UGT1A3 protein essentially abolished 1-NP and 4-MU glucuronidation, and the double T36I/P40H mutation (i.e., UGT1A3-4) in UGT1A4 abolished LTG and TFP glucuronidation. It is intriguing, however, that introduction of the single H40P (but not I36T) mutation in UGT1A3 conferred LTG and TFP glucuronidation, whereas the single T36I (but not P40H) mutation in UGT1A4 conferred 1-NP and 4-MU glucuronidation despite the apparent importance of both positions to UGT1A3 and UGT1A4 substrate selectivity.

Mechanistic interpretation of these data are problematic in the absence of a UGT X-ray crystal structure. However, a homology model for UGT1A1, which shares approximately 72% sequence identity with UGT1A3 and UGT1A4, was generated recently using a plant glycosyltransferase, UGT71G1, as the template (Locuson and Tracy, 2007). The homology model identified His39, which aligns to His40 of UGT1A3, as the catalytic base necessary for the SN2 glucuronidation reaction (Radominska-Pandya et., 1999). This histidine is conserved in all UGT1A enzymes except UGT1A4 and, consistent with the mutagenesis data reported here for UGT1A3, substitution of His38 in UGT1A6 with alanine and glutamine abolished 4-MU glucuronidation (Ouzzine et al., 2000). It is noteworthy that the glucuronidation of tertiary amines does not require aglycone deprotonation for the SN2 mechanism to proceed, although UGT1A4 does catalyze the glucuronidation of substrates other than tertiary amines (e.g., primary/secondary amines and aliphatic alcohols, including hydroxysteroids) (Green and Tephly, 1996; Bowalgaha et al., 2007). The identity of the residue that acts as the catalytic base in these reactions is unknown. It is noteworthy, however, that the single T36I (but not P40H) mutation in UGT1A4 conferred 1-NP and 4-MU glucuronidation in the present study, and this would seem consistent with the role of an alternate catalytic base to histidine.

Secondary structure analysis and the UGT1A1 homology model predicts that residue 40 of UGT1A proteins is apparently located within a conserved $\alpha$-helix (Ouzzine et al., 2000; Locuson and Tracy, 2007). Proline is known to distort $\alpha$-helical structure, and it is possible that Pro40 of UGT1A4 alters the architecture of the active site to permit binding of tertiary amines in a catalytically favorable orientation. It is noteworthy that the H40P substitution in UGT1A3 conferred LTG and TFP glucuronidation activity to UGT1A3. However, substitution of threonine at residue 36, which is critical for

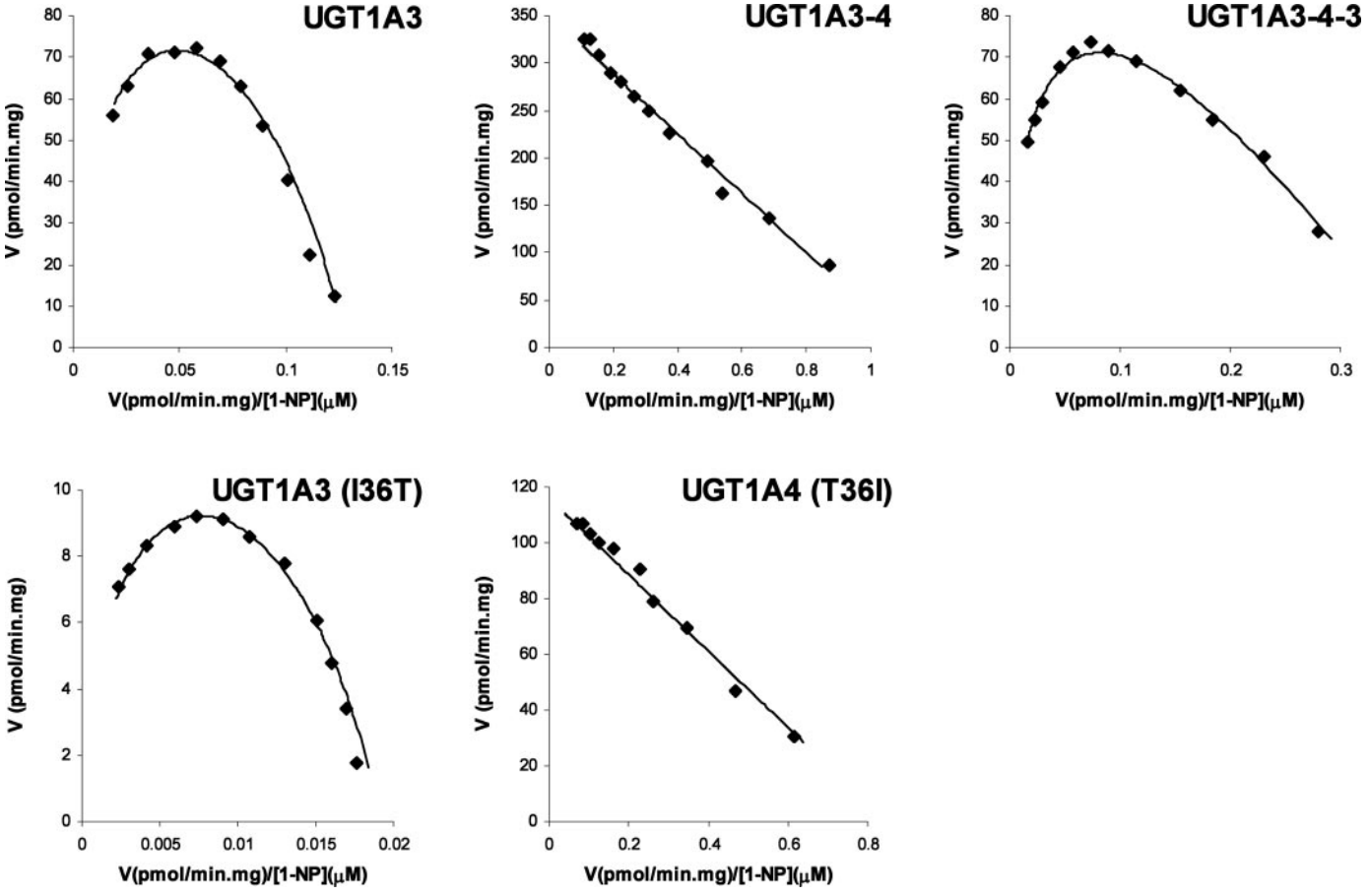


**Fig. 6.** Eadie-Hofstee plots for 1-NP glucuronidation by UGT1A3, UGT1A3-4, UGT1A3-4-3, UGT1A3(I36T), and UGT1A4(T36I). Points show experimentally determined values (mean of duplicate estimates), whereas curves are the computer-generated curves of best fit.

tertiary amine glucuronidation by UGT1A4, did not confer LTG and TFP glucuronidation activity to UGT1A3.

Reciprocal mutagenesis has previously been used to explore the differing hydroxysteroid glucuronidation substrate profiles of UGT2B15 and UGT2B17, which share 95% sequence identity (Dubois et al., 1999). UGT2B15 preferentially glucuronidates 17$\beta$-hydroxysteroids, whereas UGT2B17 metabolizes both 3$\alpha$- and 17$\beta$- hydroxysteroids. Mutation of Ser121 of UGT2B17 to tyrosine, the corresponding residue at this position in UGT2B15, abolished androsterone 3$\alpha$-glucuronidation without affecting the 17$\beta$-glucuronidation of dihydrotestosterone. In parallel with certain of the observations in the present work, the reverse mutation (Y121S) in UGT2B15 did not confer 3$\alpha$-glucuronidation activity.

Genetic variants of UGT1A3 and UGT1A4 that alter glucuronidation activity have been reported (Ehmer et al., 2004; Iwai et al., 2004; Mori et al., 2005; Chen et al., 2006). Several of these mutations are in close proximity to residues 36 and 40: R45W and V47A of UGT1A3 and L48V of UGT1A4. Although enzyme activity was variably increased or decreased, none of the mutations abolished glucuronidation by UGT1A3 or UGT1A4 (including tertiary amine glucuronidation in the case of the UGT1A4 L48V substitution).

Atypical, or non–Michaelis-Menten, kinetics has been reported for several glucuronidation reactions (e.g., Stone et al., 2003; Uchaipichat et al., 2004). Here, only LTG glucuronidation by UGT1A4 followed Michaelis-Menten kinetics. 1-NP and 4-MU glucuronidation by UGT1A3 and TFP glucuronidation by UGT1A4 exhibited kinetics characteristic of substrate inhibition. However, kinetic models and derived parameters ($K_m$, $S_{50}$, $V_{max}$, $CL_{int}$, $CL_{max}$) for the same substrate tended to vary between the parent enzyme, chimeras, and mutants. For example, Michaelis-Menten kinetics were observed for LTG glucuronidation by UGT1A4, UGT1A4-3, and UGT1A3(H40P), whereas the same reaction catalyzed by UGT1A4(P40H) and UGT1A4-3-4 exhibited substrate inhibition and sigmoidal kinetics, respectively. Despite retention of substrate selectivity, these data indicate that differences in active site architecture that affect substrate binding and/or turnover, including the ability to bind multiple substrate molecules, occur between the parent enzymes, chimeras, and mutants. Data presented here do not preclude catalytically unfavorable binding of LTG/TFP and 4-MU/1-NP in the respective UGT1A3 and UGT1A4 active sites (or to the chimeras and mutants that lack either of these glucuronidation activities). However, this study aimed to identify residues in UGT1A3 and UGT1A4 that are critical for the glucuronidation of planar phenols and tertiary amines, respectively, and hence inhibition studies were not conducted.

Previous studies (e.g., Dubois et al., 1999; Coffman et al., 2003; Xiong et al., 2006; Lewis et al., 2007) have generally linked the aglycone substrate selectivity of individual UGT enzymes with residues or domains spanning positions 60 to 194. The present study demonstrates that residues 36 and 40 of UGT1A3 and UGT1A4, which are close to the amino terminus of the mature UGT protein, are pivotal for the respective selectivities of these enzymes toward planar phenols and tertiary amines. As might be expected, however, changes in the kinetics of aglycone glucuronidation observed between the parent enzymes and the active UGT1A3/4 chimeras indicate that other regions of the proteins influence binding affinity and/or turnover. It was further shown that reciprocal mutagenesis at position 40 of UGT1A3 and position 36 of UGT1A4 resulted in reversal of aglycone substrate selectivity. This is the first demonstration of reversal of substrate selectivity between UGT enzymes by single amino acid substitutions.





**References**


Bowalgaha K, Elliot DJ, Mackenzie PI, Knights KM, and Miners JO (2007) The glucuronidation of $\Delta^4$-3-keto C19 and C21- hydroxysteroids by human liver microsomal and recombinant UDP-glucuronosyltransferases (UGTs): 6$\alpha$- and 21- hydroxyprogesterone are selective substrates for UGT2B7. *Drug Metab Dispos* **35:** 363–370.

Chen Y, Chen S, Li X, Wang X, and Zeng S (2006) Genetic variants of human UGT1A3: functional characterization and frequency distribution in a Chinese Han population. *Drug Metab Dispos* **34:**1462–1467.

Coffman BL, Kearney WR, Goldsmith S, Knosp BM, and Tephly TR (2003) Opioids bind to the amino acids 84 to 118 of UDP-glucuronosyltransferase UGT2B7. *Mol Pharmacol* **63:**283–288.

Dubois SG, Beaulieu M, Levesque E, Hum DW, and Belanger A (1999) Alteration of human UDP-glucuronosyltransferase UGT2B17 regio-specificity by a single amino acid substitution. *J Mol Biol* **289:**29–39.

Ehmer U, Vogel A, Schutte JK, Krone B, Manns MP, and Strassburg CP (2004) Variation of hepatic glucuronidation: novel functional polymorphisms of the UDP-glucuronosyltransferase UGT1A4. *Hepatology* **39:**970–977.

Green MD, King CD, Mojarrabi B, Mackenzie PI, and Tephly TR (1998) Glucuronidation of amines and other xenobiotics catalyzed by expressed human UDP-glucuronosyltransferase 1A3. *Drug Metab Dispos* **26:**507–512.

Green MD and Tephly TR (1996) Glucuronidation of amines and hydroxylated xenobiotics and endobiotics catalyzed by expressed human UGT1.4 protein. *Drug Metab Dispos* **24:**356–363.

Green MD and Tephly TR (1998) Glucuronidation of amine substrates by purified and expressed UDP-glucuronosyltransferase proteins. *Drug Metab Dispos* **26:**860–867.

Guillemette C (2003) Pharmacogenomics of human UDP-glucuronosyltransferase enzymes. *Pharmacogenomics J* **3:**136–158.

Houston JB and Kenworthy KE (2000) In vitro-in vivo scaling of CYP kinetic data not consistent with the classical Michaelis-Menten model. *Drug Metab Dispos* **28:**246–254.

Iwai M, Maruo Y, Ito M, Yamamoto K, Sato H, and Takeuchi Y (2004) Six novel UDP-glucuronosyltransferase 1A3 (UGT1A3) polymorphisms with varying activity. *J Hum Genet* **49:**123–128.

Kiang TKL, Ensom MHH, and Chang TKH (2005) UDP-Glucuronosyltransferases and clinical drug-drug interactions. *Pharmacol Ther* **106:**97–132.

Lewis BC, Mackenzie PI, Elliot DJ, Burchell B, Bhasker CR, and Miners JO (2007) Amino terminal domains of human UDP-glucuronosyltransferases (UGT) 2B7 and 2B15 associated with substrate selectivity and autoactivation. *Biochem Pharmacol* **73:**1463–1473.

Li Q, Lou XJ, Peyronneau MA, Straub PO, and Tukey RH (1997) Expression and functional domains of rabbit liver UDP-glucuronosyltransferase 2B16 and 2B13. *J Biol Chem* **272:**3272–3279.

Locuson CW and Tracy TS (2007) Comparative modelling of the human UDP-glucuronosyltransferases: insights into structure and mechanism. *Xenobiotica* **37:** 155–168.

Mackenzie PI (1990) Expression of chimeric cDNAs in cell culture defines a region of UDP glucuronosyltransferase involved in substrate selection. *J Biol Chem* **265:** 3432–3435.

Mackenzie PI, Bock KW, Burchell B, Guillemette C, Ikushiro S, Iyanagi T, Miners JO, Owens IS, and Nebert DW (2005) Nomenclature update for the mammalian UDP glycosyltransferase (UGT) gene superfamily. *Pharmacogenet Genomics* **15:** 677–685.

Martineau I, Tchernof A, and Belanger A (2004) Amino acid residue Ile211 is essential for the enzymatic activity of human UDP-glucuronosyltransferase 1A10 (UGT1A10). *Drug Metab Dispos* **32:**455–459.

Miners JO and Mackenzie PI (1991) Drug glucuronidation in humans. *Pharmacol Ther* **51:**347–369.

Miners JO, McKinnon RA, and Mackenzie PI (2002) Genetic polymorphisms of UDP-glucuronosyltransferases and their functional significance. *Toxicology* **181:** 453–456.

Miners JO, Smith PA, Sorich MJ, McKinnon RA, and Mackenzie PI (2004) Predicting human drug glucuronidation parameters: application of in vitro and in silico modeling approaches. *Annu Rev Pharmacol Toxicol* **44:**1–25.

Mojarrabi B, Butler R, and Mackenzie PI (1996) cDNA cloning and characterization of the human UDP glucuronosyltransferase, UGT1A3. *Biochem Biophys Res Commun* **225:**785–790.

Mori A, Maruo Y, Iwai M, Sato H, and Takeuchi Y (2005) UDP-glucuronosyltransferase 1A4 polymorphisms in a Japanese population and kinetics of clozapine glucuronidation. *Drug Metab Dispos* **33:**672–675.

Ouzzine M, Antonio L, Burchell B, Netter P, Fournel-Gigleux S, and Magdalou J (2000) Importance of histidine residues for the function of the human liver UDP-glucuronosyltransferase UGT1A6: evidence for the catalytic role of histidine 370. *Mol Pharmacol* **58:**1609–1615.

Radominska-Pandya A, Czernik PJ, Little JM, Battaglia E, and Mackenzie PI (1999) Structural and functional studies of UDP-glucuronosyltransferases. *Drug Metab Rev* **31:**817–899.

Ritter JK, Chen F, Sheen YY, Tran HM, Kimura S, Yeatman MT, and Owens IS (1992) A novel complex locus UGT1 encodes human bilirubin, phenol, and other

UDP-glucuronosyltransferase isozymes with identical carboxyl termini. *J Biol Chem* **267:**3257–3261.
Rowland A, Elliot DJ, Williams JA, Mackenzie PI, Dickinson RG, and Miners JO (2006) In vitro characterization of lamotrigine N2-glucuronidation and the lamotrigine-valproic acid interaction. *Drug Metab Dispos* **34:**1055–1062.
Senay C, Jedlitschky G, Terrier N, Burchell B, Magdalou J, and Fournel-Gigleux S (2002) The importance of cysteine 126 in the human liver UDP-glucuronosyltransferase UGT1A6. *Biochim Biophys Acta* **1597:**90–96.
Stone AN, Mackenzie PI, Galetin A, Houston JB, and Miners JO (2003) Isoform selectivity and kinetics of morphine 3-and 6-glucuronidation by human UDP-glucuronosyltransferases: evidence for atypical glucuronidation kinetics by UGT2B7. *Drug Metab Dispos* **31:**1086–1089.
Tukey RH and Strassburg CP (2000) Human UDP-glucuronosyltransferases: metabolism, expression, and disease. *Annu Rev Pharmacol Toxicol* **40:**581–616.
Uchaipichat V, Mackenzie PI, Elliot DJ, and Miners JO (2006) Selectivity of substrate (trifluoperazine) and inhibitor (amitriptyline, androsterone, canrenoic acid, hecogenin, phenylbutazone, quinidine, quinine, and sulfinpyrazone) "probes" for human UDP- glucuronosyltransferases. *Drug Metab Dispos* **34:**449–456.
Uchaipichat V, Mackenzie PI, Guo XH, Gardner-Stephen D, Galetin A, Houston JB, and Miners JO (2004) Human UDP-glucuronosyltransferases: isoform selectivity and kinetics of 4-methylumbelliferone and 1-naphthol glucuronidation, effects of organic solvents, and inhibition by diclofenac and probenecid. *Drug Metab Dispos* **32:**413–423.
Udomuksorn W, Elliot DJ, Lewis BC, Mackenzie PI, Yoovathaworn K and Miners JO (2007) Influence of mutations associated with Gilbert and Crigler-Najjar type II syndromes on the glucuronidation kinetics of bilirubin and other UDP-glucuronosyltransferase 1A (UGT1A) substrates. *Pharmacogenet Genomics*, in press.
Xiong Y, Bernardi D, Bratton S, Ward MD, Battaglia E, Finel M, Drake RR, and Radominska-Pandya A (2006) Phenylalanine 90 and 93 are localized within the phenol binding site of human UDP-glucuronosyltransferase 1A10 as determined by photoaffinity labeling, mass spectrometry, and site-directed mutagenesis. *Biochemistry* **45:**2322–2332.

**Address correspondence to:** Professor John Miners, Department of Clinical Pharmacology, Flinders Medical Centre, Bedford Park, SA 5042, Australia. E-mail: john.miners@flinders.edu.au